

How cite this article:

Daniel M. Michalk, Adrian R. Muxworthy, Harald N. Böhnel, John Maclennan, Norbert Nowaczyk (2008) Evaluation of the multispecimen parallel differential pTRM method: a test on historical lavas from Iceland and Mexico , *Geophysical Journal International* 173 (2) , 409–420 doi:10.1111/j.1365-246X.2008.03740.x

Evaluation of the multispecimen parallel differential pTRM method: A test on historical lavas from Iceland and Mexico

Daniel M. Michalk^{a,*}

Adrian R. Muxworthy^b

adrian.muxworthy@imperial.ac.uk

Harald N. Böhnel^c

hboehnel@dragon.geociencias.unam.mx

John Maclennan^d

jmac05@esc.cam.ac.uk

Norbert Nowaczyk^a

nowa@gfz-potsdam.de

^a*GeoForschungsZentrum Potsdam, Section 3.3, Telegrafenberg, 14473 Potsdam, Germany*

^b*Department of Earth Science and Engineering, Imperial College London, South Kensington Campus, London SW7 2AZ, U.K.*

^c*Centro de Geociencias, UNAM-Campus Juriquilla, Queretaro 76230, Mexico*

^d*Department of Earth Science, University of Cambridge, Downing Street, Cambridge, CB2 3EQ, UK*

* Daniel M. Michalk

GeoForschungsZentrum Potsdam

Section 3.3

Telegrafenberg, A58

D-14473 Potsdam

Germany

Email: michalk@gfz-potsdam.de

Summary

Obtaining reliable geomagnetic palaeointensity (PI) estimates is still a difficult objective. Most common techniques in PI studies are based on various modifications of the Thellier method, but high failure rates and large uncertainties are common. Furthermore, only rocks which obey stringent criteria are assumed to yield faithful palaeointensity estimates. In general, magnetic particles must be of single domain size, the magnetisation must be a thermoremanent magnetisation and chemical alteration of magnetic carriers must be avoided during the laboratory experiment. Recently, a new method for obtaining palaeointensities was proposed, which, on the grounds of results from two historic lavas and three simulated experiments, is assumed to be independent of magnetic domain state. This method uses multiple samples subjected to only one heating step at moderate temperatures. Here we present a test of the multispecimen parallel differential pTRM method on 11 historical lavas from Iceland and Mexico, from which the actual field intensity is known, either from magnetic observatory data, or from magnetic field models. Our results show, that the majority of PI estimates after the multispecimen parallel differential pTRM method yielded results that are very close or indistinguishable within the range of error from the expected intensity and thus largely confirm the findings from the initial study, however, there is in general a small overestimate, which we show is associated with multidomain material. When compared to a Thellier-type palaeointensity experiment, carried out on sister samples from five Icelandic lava flows, the average multispecimen PI is closer to the actual field intensity. Samples from one lava, characterized by low Curie temperatures, failed the Thellier approach due to laboratory induced alteration, but here the multispecimen method returned a reasonable PI. Even though there is evidence that the method is not entirely independent of magnetic domain state, as previously proposed, we regard this method as a valuable alternative in future PI studies.

Keywords: palaeointensity, remagnetization

1. Introduction

To understand the origin of the earth's magnetic field, we need to know how the field has varied on geological timescales; not just the direction but also the ancient field's absolute intensity (palaeointensity). This absolute palaeointensity (PI) record is particularly important, because when palaeomagnetic data are only directional this leads to non-linear calculations of the ancient geomagnetic field, whereas, if the absolute palaeointensity is known, the problem becomes linear and analytically solvable. Absolute PI data provide constraints for various numerical dynamo models, and information about the geodynamo processes and its evolution over geological timescales. Many workers have attempted to determine full vector records of the ancient geomagnetic field, however, current methods of PI determination have high failure rates and often the reliability of the PI estimate is unknown. As a result, the global data base of palaeointensities (Perrin & Schnepp, 2004) gives a rather scattered image and still remains sparse both temporally and spatially.

Generally, the high failure rates and accompanying large uncertainties of PI data are due to a number of effects, including (1) chemical alteration of magnetic minerals in situ, e.g., low temperature oxidation (magnetization), (2) chemical alteration during repeated heating in the laboratory PI determination, (3) differences between natural and laboratory cooling rates, and (4) the presence of remanence carried by multidomain (MD) grains that violate Thelliers' law of independence of partial thermoremanence (pTRM) (Thellier & Thellier, 1959), an essential criterion in any Thellier-type PI study. Many scientists have attempted to account for, or minimize the effects of these factors by applying different sets of strict, often time consuming, reliability criteria and measurements (e.g. Perrin, 1998; Selkin & Tauxe, 2000;

Riisager & Riisager, 2001). As a result the number of samples, which are considered to be suitable PI recorders, is limited to a small fraction of the original, as MD grains are commonly present and chemical alteration during the experimental procedure is also common.

Recently, Dekkers & Böhnell (2006) have presented a new method of determining palaeointensities; the multispecimen parallel differential pTRM method (hereafter referred to as multispecimen method). They claim that this method is independent of magnetic domain state, allowing for samples containing MD grains to be processed. The method requires heating to only low / moderate temperatures in the laboratory. Consequently, failure due to chemical alteration is greatly reduced.

The basic assumption that underlies the method proposed by Dekkers & Böhnell (2006) is the first-order symmetry properties of pTRM in MD ferromagnetic grains, experimentally observed by Biggin & Poidras (2006a). They found that partial demagnetisation and remagnetisation of MD TRM, displays first-order mirror-reflected symmetry in the change in magnetisation, in a similar fashion to that displayed by and expected for non-interacting SD grains (Néel, 1949). One conclusion of their phenomenological model is that if a MD sample has a full TRM and a pTRM is induced parallel to the TRM, the intensity of the resultant remanence (pTRM and original TRM) will equal the original TRM, if the laboratory field is equal to the inducing field of the TRM. If the laboratory field is less than the inducing field, the overall remanence will decrease, if greater, the overall remanence will increase. Therefore, simply plotting the resultant remanence minus the original TRM, for a range of field values, say 10-100 μT , yields the original intensity.

Dekkers & Böhnel (2006) applied this concept to the development of their new multispecimen method. In contrast to the most common methods of PI determination, which are based on modifications on Thellier-type methods, this multispecimen approach requires the use of multiple samples. Each sample is subjected to only one in-field low/moderate-temperature heating step. That each sample is heated only once is thought to significantly reduce from the effects of laboratory alteration. In addition, according to the model of Biggin & Poidras (2006a), during pTRM acquisition it is important to apply the magnetic field during both the warming and cooling.

Dekkers & Böhnel (2006) tested this new method on natural and synthetic MD grain assemblages induced with a laboratory TRM with a known field, and on only two historical lavas from the Trans Mexican Volcanic Belt (TMVB). The synthetic samples returned the correct result within error. The same samples failed to yield correct PI estimates using a double-heating Thellier method. One mean result, based on three PI experiments, obtained from the 1943-1952 Paricutin lava yielded a PI, which is statistically indistinguishable within the range of error of the expected intensity. Another result from samples belonging to the 1759-1774 Jorullo lava was of lower quality but still close to the expected intensity. In addition to these encouraging experimental tests, the laboratory processing time of the multispecimen approach is significantly faster (about 2-4 times) than Thellier-type determinations. According to Dekkers & Böhnel (2006) the multispecimen method has the potential to supersede standard Thellier-type techniques, however, the method has produced only one accurate determination from two historical lavas.

In this paper we present a test of the multispecimen method on 11 recent historical lavas of known ages from Iceland and Mexico, with a range of different well-defined rock-magnetic characteristics. We compare the palaeointensity results from our experiments with the expected intensity, known from magnetic observatory data or magnetic field models (Jackson et al., 2000). This study allows us to estimate the feasibility of using this method for routine palaeointensity determinations. We directly compare the multispecimen estimates with Thellier-type PI determinations performed on sister samples from five lavas flows.

2. Sample description

We considered historical samples from both Iceland and Mexico (Table 1). Icelandic samples are associated with eruptions from two Icelandic volcanoes; five lava flows (1878, 1913, 1980, 1991 and 2000 A.D.) from Mount Hekla in southwest Iceland, and two lava flows (1729 and 1981 A.D.) from Mount Krafla in the northeast of Iceland. The Krafla samples were taken from the two most recent basaltic fissure eruptions in the Krafla volcanic system. This system is dominated by the eruption of tholeiitic basalts which form by adiabatic decompression melting of unusually hot mantle under a spreading center. In contrast, the transitional basalts that are parental to the Hekla system are generated by mantle melting under a southwards-propagating rift segment. The north Atlantic has been the site of frequent volcanic activity through much of the Cenozoic, and on-land exposures in Iceland preserve a superb archive of the last 16 Myr of geomagnetic history (Wilson et al., 1972).

The volcanism of the TMVB is related to the Neogene subduction of the Cocos and Rivera Plates under the south-western margin of the North American Plate. It comprises at least 8000 volcanic structures and crosses Mexico at latitudes from ~19 to 21°N and extends approximately over 1000 km from the Pacific Ocean to the Gulf of Mexico with a width of 20-150 km. For this study, we sampled four historic lavas; one from the 1943 lava flow of Paricutin (active period: 1943-1952), two eruptions from Ceboruco volcano (1870 and 1550 respectively) and Pico de Orizaba (1545) (also known as Citlaltépetl), which is at 5610 m the highest volcano in Mexico. Our Paricutin site (BK) is a direct re-sampling of the locality "Paricutin site 2" from the initial study of Dekkers & Böhnel (2006). Paricutin, the youngest cinder cone of the

TMVB and belongs to the Michoacan-Guanajuato Volcanic Field. Ceboruco lies in the Ceboruco-San Pedro Volcanic Field while Pico de Orizaba is part of the TMVB.

A set of 10 to 15 oriented mini-core samples with a diameter of 11 mm for the Icelandic samples and 12 mm for the Mexican samples were taken from each cooling unit with a battery powered electric drill. Due to the very fresh nature of the Icelandic lavas, penetration into the lava field was typically less than 300 m. Effort was made to sample original, un-rotated cooling structures, such as lava tubes. Where possible, multiple structures were sampled within a radius of < 50 m. This was also the case for the Mexican samples, except for site DY. Here, the lava flow had an *in situ* exposure of ~ 15 m over which the samples were dispersed vertically and horizontally.

3. Experimental techniques

In the laboratory, samples were cut into specimens of 10 mm length, after scraping the outermost 1-1.5 cm, which then yielded two to five specimens for each drill core. To minimize the risk of using samples that might have been affected by surface weathering, we preferably used the specimens closer to the bottom of the core in the laboratory experiments. To test for their demagnetisation behaviour, e.g. univectorial remanences or possible viscous overprinting, we subjected sets of five specimens from each flow unit to progressive alternating field (AF) demagnetisation with maximum fields of 150 mT. Additionally two samples were subjected to thermal demagnetisation to obtain the blocking temperature spectrum of the NRM. Low-field susceptibility (χ) was measured on a Bartington susceptibility meter to detect chemical alteration during heating. Remanence measurements were made either on a 2G cryogenic magnetometer with long core setup or on an Agico JR6 spinner magnetometer. For thermal demagnetisation and PI experiments, we used a temperature and field calibrated Magnetic measurements Ltd. MMTD oven. The field was calibrated to an accuracy of $\pm 0.1 \mu\text{T}$ along the length of the heating chamber.

A set of rock magnetic measurements was performed on selected samples from each flow to ascertain the magneto-mineralogy and to assess for possible thermal alteration. Thermomagnetic curves were measured on five samples per flow with a Petersen Instruments Variable Field Translation Balance (VFTB) from room temperature to 600° C with Argon flushing, using a field of 500 mT. Curie temperatures were calculated after the method of Moskowitz (1981). For detailed monitoring of possible alteration effects, two samples per flow were additionally subjected to thermal cycling with 100°C steps, starting at room temperature up to the

highest temperature of 600°C. For each flow a set of three to six hysteresis measurements and back field curves were made on small chips of 30-50 mg using a Princeton measurements alternating gradient magnetometer (AGM), with a peak field of 1 Tesla. From these data sets, we determined the standard hysteresis parameters, i.e., saturation magnetisation, M_S , saturation remanence, M_{RS} , coercive force, B_C , and coercivity of remanence, B_{CR} . Using the ratios M_{RS}/M_S and B_{CR}/B_C a Day-plot was created (Day et al. 1977; Fig 2). We also calculated the shape parameter δ_{Hys} (Fabian, 2003). Additionally first-order reversal curves (FORCs) (Roberts et al., 2000) were measured on a selection of samples to identify the degree of magnetostatic interactions.

Two different techniques were used to determine the palaeointensity. Firstly, PI measurements by the multispecimen method following the protocol of Dekkers & Böhnel (2006). A basic requirement of the multispecimen method is that after each in-field pTRM acquisition treatment, the pTRM is scaled to the original NRM to determine the fraction of pTRM lost / gained (%). If scaled to the NRM, the remanence must be uni-vectorial, or, in the case of viscous overprints, the characteristic remanent magnetisation (ChRM) must be isolated before the PI experiment by a preceding demagnetisation treatment. Previous AF-demagnetisation experiments on sister samples indicated for three lavas (sites H00, H91 and HG) that a field of 5 mT was required to erase a small viscous overprint, while for one set of samples (site DY) it was necessary to apply a slightly higher field of 10 mT. Dekkers & Böhnel (2006) used a thermal pre-treatment of a 200°C demagnetisation step on one set of samples from Jorullo. We used an AFD pre-treatment as we suggest that AF-demagnetisation at such low fields is a sufficient tool for erasing small fractions of viscous magnetisations and that each additional thermal treatment would rather

increase the risk of inducing laboratory alteration effects. In the multispecimen PI determination, these four samples were AF-demagnetised after each remagnetisation step for normalisation purposes. For all the other samples the magnetisation was found to be uni-vectorial and free of viscous components and consequently pTRMs were scaled to the NRM.

During the experiments, pTRMs were induced parallel to the original NRM to avoid effects of high temperature tails of multidomain pTRMs (Yu & Dunlop, 2003; Xu & Dunlop, 2004). As it was possible to orient ChRM of the samples parallel to the induced field in a special designed sample holder with a precision of less than $<10^\circ$, no later mathematical correction, to account for inaccuracies in orientation, was required on the final data. Ideally, in a multispecimen experiment, the unblocking temperature spectrum (T_{UB}) of all specimens used in one experiment should be the same. We included one more demagnetisation step in zero-field at the same temperature at which the pTRM was acquired after the pTRM acquisition, i.e. similar to a pTRM tail check (e.g. Walton, 1984; McClelland & Briden, 1996). We used this as a criterion to further characterize the T_{UB} spectrum of each sample. We discarded measurements with anomalous values of NRM remaining after demagnetisation. For the multispecimen experiment it is necessary to select a temperature for the pTRM acquisition, which is below the point where chemical alteration is significant and above where viscous components persist. The temperature was chosen high enough that the fraction of TRM lost after heating in zero-field was in the order of 30-60% and increases in magnetic susceptibility were less than 5%.

We applied successively increasing fields in 10 μT steps from 10 μT to 80 μT , sometimes 90 μT . After each remagnetisation experiment, the bulk susceptibility was measured.

In conjunction and for comparison with the multispecimen PI experiments, we subjected a set of sister samples from five Icelandic flows to a Thellier-type palaeointensity experiment. We used the IZZI protocol described by Tauxe & Staudigel (2004) and Yu et al. (2004). We included both pTRM checks and pTRM tail checks as described by Yu et al. (2004). No pTRM additivity checks (Krása et al., 2003) were measured.

4. Rock magnetic analysis

4.1 Thermomagnetic properties

Thermomagnetic results from the VFTB are categorized into four groups (Fig. 1, Table 2). Group 1 samples (Fig. 1a) show a single ferromagnetic phase with a broad Curie temperature (T_C) between 390 and 460°C, which is likely to be due to titanomagnetite that has undergone some degree of high temperature (deuteric) oxidation. Heating and cooling branches show excellent reversibility, indicating that no thermal alteration occurs. This behaviour was observed in samples from sites DY and BK.

Group 2 samples (Figs 1b and c) are characterized by two ferromagnetic phases. Phase one has a low T_C in the range of 180 to 220°C, which is indicative of high-Ti titanomagnetite, the second phase has a higher T_C between 510 and 560°C, indicative of low-Ti titanomagnetite. Both Curie temperatures are seen in the heating and cooling curve, which again show reversible behaviour. Such thermomagnetic curves were observed in the majority of samples (Table 2).

Group 3 samples (sites HG and KB, Figs 3d and e) show a range of different Curie temperatures rather than a single pronounced Curie temperature, and again the behaviour is reversible.

Samples from site KA are categorized as Group 4 samples (Fig. 3f) and show a dominant ferromagnetic phase with a T_C between 105 and 140°C, which indicates the presence of high-Ti titanomagnetite phase close to TM60 in composition, suggesting fast cooling of the lava before high-temperature oxidation could occur

(Mankinen et al., 1985). In these samples, thermal cycling above 400°C shows progressive irreversibility in the cooling curve, which is likely to be due to progressive inversion of titanomaghemite during laboratory heating (i.e., Krasa & Matzka, 2007). The final product is a magnetic phase with a $T_C \sim 580^\circ\text{C}$ close to that of pure magnetite.

4.2 Hysteresis properties

The bulk magnetic hysteresis properties for the Icelandic and Mexican samples is shown in Figure 2 and tabulated in Table 2. The majority of Icelandic samples (indicated by dots) have average values of M_{RS}/M_S of 0.45-0.26 and B_{CR}/B_C values of 1.49-1.37 and plot in the upper left corner of the pseudo-single domain (PSD) range in the Day diagram. Two lavas (H00 and H91) have slightly lower values of M_{RS}/M_S and higher values of B_{CR}/B_C . FORC diagrams show closed contours about a central peak, which are typical for SD particle assemblages (Figs 3a and b). The presence of a negative region or a low in the FORC distribution near the bottom left-hand region in these FORC diagrams is highly indicative of non-interacting SD material with a dominant uniaxial anisotropy (Muxworthy et al., 2004; Newell, 2005), i.e., ideal material for recording the PI.

Hysteresis properties of the Mexican samples (indicated as squares) show a broader range of magnetic domain states. While samples from BK show a similar behaviour like the majority of the Icelandic samples (Fig. 3c), and site EH samples still plot well in the PSD region, samples from DY and EE are characterized by rather lower values of M_{RS}/M_S (0.09 and 0.11) and higher values of B_{CR}/B_C (4.68 and 5.05), which indicates some contribution of multidomain (MD) grains. This can be more clearly seen in the FORC diagrams (Figs 5d-f), which plot closer to the vertical axis and display a greater vertical spread in the distribution along the B_i -axis. This is similar to published FORC diagrams for PSD powdered magnetite (Muxworthy & Roberts, 2007).

5. Palaeointensity experiments

5.1 Multispecimen PI

Figure 4 shows the results of the multispecimen PI experiments per site. At eight sites we used nine samples, i.e., nine applied fields, and for four sites, eight samples for each experiment. As stated in 3, the multispecimen method relies on the temperature selected for pTRM acquisition at which the field is applied during heating and cooling. Because of the large variations in unblocking spectra determined from sister samples and thermomagnetic curve analyses (Figure 1, Table 2), we used five different temperatures for the pTRM acquisition step: 130°C (sites KA and KB), 200°C (sites H00, HB, EH), 280°C (sites H00, HG and BK), 300°C (sites HE and EE) and 400°C (site DY).

For comparison of the measured palaeointensity (I_{meas}) with the expected palaeointensity (I_{exp}), we use the intensity error fraction (IEF) equation,

$$(1) \quad IEF = (I_{meas} - I_{exp}) / I_{exp}$$

For the post 1900 flows, expected intensity values were deduced from the International Geomagnetic Reference Field (IGRF), and for the pre-1900 flows, they were calculated using the GUFM1 model (Jackson et al., 2000). The GUFM model assumes a 15 nT/yr decrease in dipole moment in its pre-1840 intensity estimates. As this model only extends back to 1590, intensity values for the two flows pre-dating 1590 (sites EE and DY), were calculated by extrapolating back using secular variation rates provided from the GUFM model for 1590 (Table 3).

5.1.1 Icelandic samples

For site H00, we had sufficient material to conduct two PI measurements (Fig. 4a and b) at two different temperatures (280° and 200°C respectively). For the experiment at 280°C we used an AF-demagnetisation pre-treatment as described in 3, while for the experiment at 200°C remanences were scaled to the NRM. The pTRM induced at 280°C gave a PI estimate of $60 \pm 5 \mu\text{T}$ ($R^2= 0.86$, IEF= $+15 \pm 10\%$), whilst the pTRM induced at the lower temperature of 200°C and gave a PI of $61 \pm 6 \mu\text{T}$ ($R^2= 0.83$, IEF= $+17 \pm 12\%$). As expected, the curve for the 200°C experiment has a slightly flatter slope than for the 280°C experiment because a smaller fraction of NRM is removed at 200° than at 280°C. Both the correlation coefficients R^2 have similar values and based on statistical results, palaeointensities are indistinguishable from one another. A minor improvement of clustering is observed in the samples subjected to the 5 mT AF pre-treatment, which could be due to randomizing small grains that might have formed during the experiment, as discussed in Bönhel & Dekkers (2006) but overall it had a negligible effect on the final result.

Site H91 (Fig. 4c) yielded a PI estimate of 48 ± 4 ($R^2= 0.79$, IEF= $-8 \pm 8\%$). This result is within the range of error indistinguishable from the expected PI of $52 \mu\text{T}$. The data is rather noisy, as indicated by the rather low R^2 value. Samples from site HB (Fig. 4d) yielded an estimate of $54 \pm 3 \mu\text{T}$, ($R^2= 0.93$, IEF= $+4 \pm 6\%$), which is also indistinguishable from the expected value of $52 \mu\text{T}$ within the range of error. Larger scatter was observed in the data of site HG (Fig. 4e). Here, the lower part of the diagram shows fairly noisy data. Due to the remagnetisation nature of the experiment, it would be expected that measurements where the pTRM field intensity is greater than the original inducing field to display less scatter, i.e., the scatter in the data will decrease as the field increases. Calculating a PI estimate from all measurements gave a PI of $57 \pm 8 \mu\text{T}$ ($R^2= 0.70$, IEF= $+10 \pm 15\%$). Samples from

site HE produced rather noisy data (Fig. 4f), but again gave a PI which is close to the expected value ($51 \pm 7 \mu\text{T}$, $R^2 = 0.72$, $\text{IEF} = -2 \pm 13\%$).

Both sites from Krafla (sites KA and KB) are characterized by low Curie temperatures and unblocking spectra; 80 % of the NRM thermally demagnetised at 150°C . A pTRM temperature of 130°C was chosen. Both experiments (Figs 4g and h) display linear behaviour with high R^2 values of 0.96 and 0.97 respectively. However, the PI estimates are rather high, at $64 \pm 3 \mu\text{T}$ and $58.8 \pm 1.2 \mu\text{T}$ respectively, with corresponding IEFs of $+23 \pm 6\%$ and $+11 \pm 2\%$.

5.1.2 Mexican samples

Our experiment on the samples from Paricutin (BK) (Fig. 4i), produced a PI of $47.1 \pm 1.4 \mu\text{T}$ ($R^2 = 0.98$, $\text{IEF} = +4 \pm 3\%$), which is very close to the expected intensity of $45 \mu\text{T}$. Dekkers & Böhnell (2006) sampled exactly the same locality (Paricutin site 2 in their publication) and obtained a result of $47.2 \pm 1.6 \mu\text{T}$. Our estimate is in excellent agreement with their data.

Site EH gave a PI estimate of $54 \pm 6 \mu\text{T}$ ($R^2 = 0.777$, $\text{IEF} = +13 \pm 12\%$, Fig. 4j).

Although this is a relatively poorly defined result, it is, within the range of error indistinguishable from the expected intensity of $48 \mu\text{T}$. Results from sites EE and DY (Figs. 4k and l), on the other hand, showed the largest overestimates from all historical lava flows investigated in this study ($65 \pm 6 \mu\text{T}$, $R^2 = 0.83$, $\text{IEF} = 30 \pm 12\%$ and $61.6 \pm 1.3 \mu\text{T}$, $R^2 = 0.98$, $\text{IEF} = 31 \pm 3\%$). Due to a sharp T_{UB} spectrum between 350 and 450°C the temperature for the pTRM acquisition for the samples from site DY was chosen with 400°C the highest from all in this study.

As stated in section 3, we subjected four lavas to an AF demagnetisation pre-treatment before the pTRM acquisition step, to erase small amounts of viscous magnetisation, and after the pTRM acquisition, for normalization purposes. No

adverse effects were found on the final outcome of the multispecimen experiment.

However, we want to emphasize that the effects of an AF pre-treatment still have to be experimentally evaluated before this approach should be considered in a multispecimen experiment on older samples of geological ages.

5.2 Thellier data

For comparison to the multispecimen PI experiments, we subjected sister samples from five Icelandic lavas (sites H00, HB, HE, HG and KB) to a Thellier-type palaeointensity experiment. We used the IZZI protocol (Tauxe and Staudigel, 2004) including pTRM checks (Coe et al., 1978) after each in-field temperature step to monitor changes in the capacity of the specimen to acquire a pTRM and alteration during laboratory treatment. Furthermore, pTRM-tail checks (e.g. Walton, 1984; McClelland & Briden, 1996) were used to test if the pTRM gained is completely removed by reheating to the same temperature step in zero-field and to estimate the importance of MD remanence. A laboratory field of 51.1 μT was used for all measurements and was applied during heating and cooling. All determinations were analyzed using the Thellier Tool 4.1 software (Leonhardt et al., 2004) applying the rigorous default quality criteria. Results from four specimens are shown in Figure 5.

Successful measurements were analyzed between room temperature or 100° and 300°/340°C over five to seven successive data points, comprising a NRM fraction f between 55 and 97%, with the exception of one sample (HE2Y, $f = 0.34$), before pTRM checks started to fail. The low-temperatures are due to the high Ti content, and resulting low Curie temperatures and low-unblocking-temperature spectra. In general a good linearity is observed on the NRM/pTRM diagrams with no zig-zagging behaviour (Tauxe & Staudigel, 2004) between alternating in-field-zero-field (IZ) and zero-field-in-field (ZI) steps. This behaviour is often interpreted as being indicative of SD remanences. In contrast, the phenomenological model of Biggin (2006b) predicts that the similar behaviour would be expected from samples containing large MD grains, if the inducing laboratory field is not aligned between perpendicular and anti-parallel to a sample's NRM direction.

From the five specimens measured from each flow, site HG yielded four estimates that passed the Thellier Tool software's reliability standards (Leonhardt et al., 2004), site H00 three, site HE two and site HB one successful determination. Experiments on samples from site KB, however, were unsuccessful due to heating induced alteration at very low temperatures, as indicated by the drift in the pTRM checks (Fig. 5d). This behaviour follows the observations made during preliminary thermal cycling as discussed in 4.1. Palaeointensity results after the IZZI method are shown in Table 4.

6. Discussion

As can be seen from Table 3, many of the actual known field values fall within the error ranges of the multispecimen PI estimates, though there is clearly a tendency towards over-estimation; 10 out of the 12 estimations are too high. Interestingly the samples from the same locality as considered by Dekkers & Böhnelt (2006) yielded one of the lowest IEF percentages. There are several possible mechanisms for this overestimation. The choice of pTRM acquisition temperature might have some effect on accuracy of the multispecimen experiment; however, for the one site (H00) where we repeated the experiment at a different acquisition temperature, both PI estimates were almost identical. Possible factors that govern overestimations of PI measurements are discussed in the following.

6.1 MD remanences as the possible cause of PI-overestimates

One possible reason for these overestimates is the presence of MD material. As stated in the introduction the multispecimen approach is based on the first-order symmetry findings of Biggen & Poidras (2006a). However, the phenomenological model of Biggen & Poidras (2006a) is not supported by the study of McClelland et al. (1996) who conducted a number of progressive re-magnetisation experiments for synthetic powders of sized MD magnetite, i.e., over-printing of TRM with successive pTRMs (field always on). In contrast to Biggen & Poidras (2006a), they found that incrementally replacing a laboratory TRM, with parallel pTRMs induced at increasing temperatures, resulted in a systematic reduction of the total intensity (Fig. 7). The original TRM was repeatable. However, it is not known how reliable the samples (provided by Dankers (1978)) used in the McClelland et al. (1996) study are, as some

of the larger samples display self-reversing behaviour (McClelland & Shcherbakov, 1995).

As a rough estimate of MD content, the ratio M_{RS}/M_S provides a crude estimate, i.e., as M_{RS}/M_S increases the material becomes more SD like. We plot IEF (%) versus M_{RS}/M_S (Fig. 6). With the exception of sample H91, it shows that there is a loose inverse correlation ($R^2 = 0.30$) between IEF (%) versus M_{RS}/M_S , i.e., as the material becomes more MD-like the overestimation in PI increases. This is particularly apparent for the two sites EE and DY, which yielded the highest overestimates (30% and 31%) and have the lowest M_{RS}/M_S ratios of ~ 0.1 . However, it is intriguing that these sites are of similar age and show similar overestimates. It has to be noted, that the high IEFs observed here may partly be due to inaccuracies in the GUFM1 model and that the resolution of the field model is too low for such a detailed comparison study. Furthermore, uncertainties due to extrapolating back from the 1590 PI + secular variation estimates (see Table 3) to obtain I_{exp} values for these sites might introduce a further bias here. The only site, which does not follow the observed trend towards overestimation of the PI, is site H91. A FORC diagram from site H91 (Fig. 3b), is characteristic of SD material, yet its M_{RS}/M_S ratio is quite low. It is likely that the dominant carrier is SD, yet there is sufficient non-SD behaving material in the sample to reduce M_{RS}/M_S .

In general, the trend observed in Figure 7 stands in contrast to the results of Dekkers & Böhnel (2006), who obtained reasonable PI estimates for a laboratory induced TRM imparted in three MD magnetite-powder samples.

6.2 Possible influences of cooling rate effects

Several studies have previously documented, that differences in cooling rates between the original remanence acquisition of a rock unit and that acquired in the laboratory, will yield erroneous PI results. In general, the TRM intensity in an assemblage of SD is positively correlated with cooling time (e.g. Fox & Aitken, 1980, McClelland-Brown, 1984, Selkin & Tauxe, 2000) and would produce rather higher palaeointensities because the cooling time in the laboratory is much faster (often not more than 30 minutes) than compared to the cooling of a lava flow in nature (up to several months). The effect of differences in the cooling rate on TRM intensity in MD and PSD assemblages is presently still a matter of debate. McClelland-Brown (1984) argued that faster cooling rates will give rise to weaker TRMs. This would cause underestimations of the PI for samples characterized by a high amount of MD particles, which is in contrast to the trend observed in Figure 6. In their comparison study of several different palaeointensity techniques, performed on samples from Mt. Etna, Biggin et al. (2007) observed rather lower PIs from samples taken from the interior of the lavas flows, when compared to the samples from the upper flow units, which supports the argument of McClelland-Brown (1984). However, the samples used in this study, all came either from flow tops or the outer margins and fronts of lava flows. Thus they are assumed to have cooled rapidly. We therefore regard the effects of cooling rate difference as negligible for the outcome of our study.

6.3 Comparison with the IZZI protocol results

In Table 3, we compare the multispecimen results with the data derived from the Thellier-type IZZI protocol. Site KB failed to pass the quality checks, and hence failed to return an IZZI PI estimate. Four sites returned a PI estimate after both methods. It is apparent, that the multispecimen method produced PI estimates closer to the actual field than the IZZI estimates and additionally returned a reasonable PI estimate for the site KB, which failed the IZZI protocol. That is, on the five lavas subjected to both methods measured in this study, the multispecimen method produced more accurate PI estimates.

There are some important points and differences between the two approaches, which require a further discussion. The Thellier-type methods have been developed, refined and tested many times, resulting in much stricter analysis and selection criteria. For the multispecimen analysis the only assessment of quality is the quality of fit of the linear regression applied to the data.

In this study, the average of the IZZI IEFs is close to zero (-0.9%). In contrast, the average IEF for the multispecimen samples (+12%) shows positive values. Yet, the average multispecimen PI is closer to the actual field intensity. A possible reason for the increase in accuracy is the number of samples, or the total amount of material used to provide the PI estimates. In the IZZI approach, many samples fail the selection criteria for reliable palaeointensity determination (i.e. at site HB, only one specimen out of five produced a reliable PI estimate). Further we observe inaccuracies of up to ~20 % on an individual sample level, even for high quality samples displaying class A behaviour. It is assumed that this would be the case for

any common Thellier-type method. It further highlights the importance, that a PI estimate should be based on the results from multiple samples, when adopting the Thellier method, i.e. $n \geq 5$, as previously proposed by Biggen et al., (2003). This is the case in the multispecimen approach because, by its very nature, it requires between eight and ten samples. Therefore, whilst the multispecimen approach provides only a single answer, the answer is based on average on more samples than used in a typical Thellier-type PI estimate from a single flow unit.

7. Conclusions

Results from this study place some important new constraints on the applicability of the multispecimen parallel differential pTRM method in future palaeointensity studies.

Results of six multispecimen PI experiments from 11 historic lava flows investigated in this study, yielded results that are very close, or indistinguishable within error from the expected intensity. This observation largely confirms the findings that were presented in the initial study of Dekkers & Böhnel (2006).

However, we observed a bias towards over-estimation because from in total 12 estimations, 10 gave values too high. The observed inverse correlation between IEF (%) versus M_{RS}/M_S , indicates that, as the material becomes more MD-like, the overestimation in PI increases. We interpret this being due to effective demagnetisation during progressive re-magnetisation, leading to an overestimate of the palaeointensity. This apparent bias in the final outcome of a multispecimen experiment implies that the method might not be entirely independent of magnetic domain state as previously proposed by Dekkers & Böhnel (2006).

On sister samples from five lavas, additional Thellier-type experiments were carried out. When compared to the corresponding multispecimen PI experiments, we found that the latter gave palaeointensity estimates that were closer to the expected intensity values. Besides showing inaccuracies of > 20 % on individual high quality samples, the Thellier-type approach had a much lower success rate in obtaining a PI estimate. Furthermore, it was not possible to process samples from one lava flow with very low Curie temperatures ($T_c = 105^\circ - 140^\circ\text{C}$) with a Thellier-type approach, due to experimentally induced alteration. Here, the multispecimen experiment was

still successful in producing one PI estimate for this site, suggesting that the multispecimen method has a higher potential in obtaining PI estimates from such critical material.

We suggest that by performing sets of different experiments at different pTRM acquisition temperatures with smaller field steps will increase statistical precision and minimize other biasing effects i.e. thermal alteration during the laboratory experiment. The issue of MD contribution to multispecimen PI estimates needs to be fully quantified, and other potential factors that might govern incomplete remagnetisation, e.g., increased internal stress, need to be experimentally evaluated.

From the majority of results obtained in this study, the multispecimen method appears to be a viable alternative for future palaeointensity studies. The significantly faster sample processing rate will open up the possibility for acquiring larger datasets of palaeointensity data. Future studies need to develop reliability tests and assess the quality of PI estimates for the multispecimen parallel differential pTRM method.

Acknowledgements

We thank Michael Winklhofer for providing the FORCobello computer program and David Gubbins for providing the GUFM1 program. Andrew Biggin and David Krása are thanked for giving some valuable comments to improve the manuscript. Much appreciated assistance during the collection of the Mexican samples came from Ivan Barajas and Gildardo Gonzalez. Collection of the Mexican samples was funded by DFG grant 334/1-2 and Conacyt grant 46213. Collection of the Icelandic samples was funded through NERC grant NE/D000351/1. ARM is funded by the Royal Society.

Reference list

Biggin, A.J., Böhnell, H.N. & Zúniga, F.R., 2003. How many palaeointensity determinations are required from a single lava flow to constitute a reliable average?, *Geophys. Res. Lett.*, **30**, NO. 11, doi:10.1029/2003GL017146.

Biggin, A.J. & Poidras, T., 2006a. First-order symmetry of weak-field partial thermoremanence in multi-domain (MD) ferromagnetic grains: 1. Experimental evidence and physical implications, *Earth Planet. Sci. Lett.*, **245**, 438-453.

Biggin, A.J., 2006b. First-order symmetry of weak-field partial thermoremanence in multi-domain (MD) ferromagnetic grains: 2 Implications for Thellier-type palaeointensity determination, *Earth Planet. Sci. Lett.*, **245**, 454-470.

Biggin, A.J., Perrin, M. & Dekkers, M.J., 2007. A reliable absolute palaeointensity determination obtained from a non-ideal recorder, *Earth Planet. Sci. Lett.*, **257**, 545-563.

Coe, R.S., Grommé, S. & Mankinen, E.A., 1978. Geomagnetic paleointensities from radiocarbon-dated lava flows on Hawaii and the question of the Pacific nondipole low, *J. Geophys. Res.*, **83**, 1740-1756.

Dankers, P. 1978. Magnetic properties of dispersed natural iron-oxides of known grain size, Ph.D. thesis, State University of Utrecht.

Day, R., Fuller, M., & Schmidt, V.A., 1977. Hysteresis properties of titanomagnetites: Grain-size and compositional dependence, *Phys. Earth Planet. Inter.*, **13**, 260-267.

Dekkers, M.J. & Böhnel, H.N., 2006. Reliable absolute palaeointensities independent of magnetic domain state, *Earth Planet. Sci. Lett.*, **248**, 507-516.

Fabian, K., 2003. Some additional parameters to estimate domain state from isothermal magnetization measurements, *Earth Planet. Sci. Lett.*, **213**, 337-345.

Fox, J.M.W., & Aitken, M.J., 1980. Cooling-rate dependence of thermoremanent magnetisation, *Nature*, **283**, 462-463.

Jackson, A., Jonkers, A.R.T., & Walker, M.R., 2000. Four centuries of geomagnetic secular variation from historical records, *Phil. Trans. R. Soc. Lond.*, **358**, 957-990.

Krása, D., Heunemann, C., Leonhardt, R., & Petersen, N., 2003. Experimental procedure to detect multidomain remanence during Thellier-Thellier experiments, *Physics and Chemistry of the Earth*. **28**, 681-687.

Krása, D., & Matzka, J., 2007. Inversion of titanomaghemite in oceanic basalt during heating, *Phys. Earth Planet. Inter.*, **160**, 169-179.

Leonhardt, R., Heunemann, C., & Krása, D., 2004. Analyzing absolute paleointensity determinations: Acceptance criteria and the software ThellierTool4.0, *Geochem. Geophys. Geosyst.*, **5**, Q12016, doi:10.1029/2004GC00807.

Mankinen, E.A., Prevot, M., Gromme, C.S., & Coe, R.S., 1985. The Steens Mountain (Oregon) geomagnetic polarity transition 1. Directional history, duration of episodes, and rock magnetism (USA). *J. Geophys. Res.*, **90**, 10 393-10 416.

McClelland-Brown, E., 1984. Experiments on TRM intensity dependence on cooling rate, *Geophys. Res. Lett.*, **11**, 205-208.

McClelland, E., & Shcherbakov, V.P., 1995. Metastability of domain state in MD magnetite: consequences for remanence acquisition, *J. Geophys. Res.*, **100(B3)**, 3841–3857.

McClelland, E., & Briden, J.C., 1996. An improved methodology for Thellier-type paleointensity determination in igneous rocks and its usefulness for verifying primary thermoremanence, *J. Geophys. Res.*, **101**, 21 995-22 013.

McClelland, E., Muxworthy, A.R., & Thomas, R.M., 1996. Magnetic properties of the stable fraction of remanence in large multidomain (MD) magnetite grains: Single-domain or MD?, *Geophys. Res. Lett.*, **23**, 2831-2834.

Muxworthy, A.R., Heslop, D., & Williams, W., 2004. Influence of magnetostatic interactions on first-order-reversal-curve (FORC) diagrams: A micromagnetic approach, *Geophys J. Int.*, **158**, 888-897.

Muxworthy, A.R., & Roberts, A.P., 2007. First-order reversal curve (FORC) diagrams, in *Encyclopedia of Geomagnetism and Paleomagnetism*, pp. 266-272, eds Herrero-Bervera, E., Gubbins, D., Springer.

Néel, L., 1949. Théorie du traînage magnétique des ferromagnétiques en grains fins avec applications aux terres cuites, *Ann. Géophys.*, **5**, 99-136.

Newell, A.J., 2005. A high-precision model of first-order reversal curve (FORC) functions for single-domain ferromagnets with uniaxial anisotropy, *Geochem. Geophys. Geosyst.*, **6**, Q05010, doi:10.1029/2004GC00877.

Perrin, M., 1998. Paleointensity determination, magnetic domain structure, and selection criteria, *J. Geophys. Res.*, **103**, 30 591-30 600.

Perrin, M. & Schnepp, E., 2004. IAGA paleointensity database: Distribution and quality of the data set, *Phys. Earth Planet. Inter.*, **147**, 255-267.

Prevot, M., Mankinen, E.A., Coe, R.S. & Gromme, C.S., 1985. The Steens Mountain (Oregon) geomagnetic polarity transition 2. Field intensity variations and discussion of reversal models (USA), *J. Geophys. Res.*, **90**, 10 417-10 448.

Riisager, P. & Riisager, J., 2001. Detecting multidomain magnetic grains in Thellier palaeointensity experiments, *Phys. Earth Planet. Inter.*, **125**, 111-117.

Roberts, A.P., Pike, C.R., & Verosub, K.L., 2000. First-order reversal curve diagrams: A new tool for characterizing the magnetic properties of natural samples, *J. Geophys. Res.*, **105**, 28 461-28 475.

Selkin, P.A. & Tauxe, L., 2000. Long-term variations in palaeointensity, *Phil. Trans. R. Soc. London*, **358**, 1065-1088.

Tauxe, L & Staudigel, H., 2004. Strength of the geomagnetic field in the Cretaceous normal superchron: New data from submarine basaltic glass of the Troodos Ophiolite, *Geochem. Geophys. Geosyst.*, **5**, Q02H06 doi: 10.1029/2003GC00635.

Thellier, E. & Thellier, O., 1959. Sur l'intensité du champ magnétique terrestre dans le passé historique et géologique, *Ann. Geophys* **15**, 285-376.

Walton, D., 1984. Re-evaluation of Greek archaeomagnitudes, *Nature*, **310**, 740-743.

Wilson, R.L., Watkins, N.D., Einarsson, T., Sigurgeirsson, T., Haggerty, S.E., Smith, P.J., Dagley, P. & McCormack, A.G., 1972. Paleomagnetism of ten lava sequences from SW Iceland, *Geophys. J. R. Astron. Soc.*, **29**, 459-471.

Xu, S. & Dunlop, D.J., 2004. Thellier palaeointensity theory and experiments for multidomain grains, *J. Geophys. Res.*, **109**, B07103, doi: 10.1029/2004JB003024.

Yu, Y. & Dunlop, D.J., 2003. On partial thermoremanent magnetization tail checks in Thellier paleointensity determination, *J. Geophys. Res.*, **108**, B11 2523, doi:10.1029/2003JB002420.

Yu, Y., Tauxe, L. & Genevey, A., 2004. Toward an optimal geomagnetic field intensity determination technique, *Geochem. Geophys. Geosyst.* **5**, Q02H07, doi: 10.1029/2003GC000630.

Figure 1. Representative examples of thermomagnetic curve types, measured with an applied field of 500 mT from room temperature to 600° (700°) C. Heating (solid line) and cooling (dashed line) was conducted in Argon. A paramagnetic correction was not necessary as the magnetisations above the highest T_C were small (generally only between 6 and less than 2 %).

Figure 2. Bulk magnetic hysteresis properties for Icelandic samples (indicated as dots) and Mexican samples (indicated as open squares), plotted on a Day diagram, using the data tabulated in Table 2.

Figure 3. Representative first order reversal curve (FORC) diagrams (normalized to peak values). a) and b) Icelandic samples and c) to f) Mexican samples. B_C corresponds roughly to the coercivity distribution in the sample, and B_i is an indicator of interaction field strength. The smoothing factors (SF) are indicated on the diagram. The measuring time for all the samples was 100 ms. Each FORC diagram was constructed from 120 FORCs.

Figure 4. Application of the multispecimen protocol to 11 historic lavas, with two estimates for the Icelandic site H00 (a and b). A linear regression is shown (dashed line) with the 68% confidence zone (one standard deviation), indicated by the longer dashed lines. The abbreviation indicates the temperature for the pTRM acquisition (e.g. H00_280, pTRM acquisition at 280°C). IEF is the intensity error fraction (%) and R^2 is the correlation coefficient of the linear regression.

Figure 5. Four examples of NRM/pTRM diagrams from Thellier-type palaeointensity experiments after the IZZI protocol on the Icelandic lavas. In a), b), and c) the straight line segment covers more than 50% of the NRM, while d) shows an unsuccessful experiment. The pTRM checks are indicated by the triangles. The inset figure to the upper right of each diagram shows the demagnetisation behaviour of the specimen on a vector component plot.

Figure 6. Intensity error fraction (IEF%) of the multispecimen PI experiments versus M_{RS}/M_S for samples considered in this study. M_{RS}/M_S is treated as an estimate of MD contribution to the bulk remanence. A linear regression ($R^2= 0.30$) is indicated by the dashed line.

Figure 7. Progressive remagnetisation of a TRM by partial replacement with a pTRM on crushed and sieved stoichiometric magnetite samples with size fractions of 5-10 μm and 30-40 μm . Redrawn from McClelland et al. (1996).

Table 1. Sample codes, origin, associated volcano, site coordinates and associated ages (A.D.).

Site	Origin	volcano	age (A.D.)	Lat. (°N)	Long. (°W)
H00	Iceland	Hekla	2000	63.9405	19.6490
H91	Iceland	Hekla	1991	63.9599	19.5952
HB	Iceland	Hekla	1980	64.0209	19.7441
HG	Iceland	Hekla	1913	63.9993	19.5109
HE	Iceland	Hekla	1878	64.0077	19.5055
KA	Iceland	Krafla	1981	65.4373	16.5127
KB	Iceland	Krafla	1729	65.4373	16.5127
BK	Mexico	Paricutin	1943	19.3163	102.1390
EH	Mexico	Ceboruco	1870	21.0967	104.5853
EE	Mexico	Ceboruco	1550	21.1755	104.5292
DY	Mexico	Pico de Orizaba	1545	19.0101	97.2910

Table 2. Average site hysteresis values for the parameters B_C , B_{CR} and M_{RS}/M_S ; δHys is the shape parameter (Fabian 2003); also shown is the thermomagnetic classification as described in 4.1 and shown in Figure 1.

site	B_C	B_{CR}	M_{RS}/M_S	δHys	Ms(T) curve type
H00	8.0 ± 1.2	14.2 ± 2.5	0.26 ± 0.04	0.12 ± 0.10	2
H91	9.9 ± 3.8	19.7 ± 4.3	0.20 ± 0.06	0.32 ± 0.21	2
HB	15.1 ± 9.4	21.5 ± 12.2	0.36 ± 0.07	0.43 ± 0.11	2
HG	26.5 ± 7.7	38.3 ± 7.0	0.43 ± 0.07	0.11 ± 0.05	3
HE	34.4 ± 2.9	48.0 ± 5.4	0.44 ± 0.02	0.24 ± 0.08	2
KA	15.2 ± 4.0	21.0 ± 6.4	0.34 ± 0.08	0.46 ± 0.17	4
KB	14.1 ± 2.3	20.7 ± 3.2	0.37 ± 0.06	0.22 ± 0.13	3
BK	14.7 ± 6.3	21.4 ± 7.8	0.33 ± 0.09	0.17 ± 0.13	1
EH	8.3 ± 1.6	25.2 ± 2.5	0.18 ± 0.04	0.02 ± 0.16	2
EE	6.3 ± 1.4	31.0 ± 7.6	0.11 ± 0.02	0.14 ± 0.15	2
DY	8.1 ± 2.7	35.4 ± 4.2	0.09 ± 0.03	0.30 ± 0.12	1

Table 3. Average PI results from the Thellier-type experiment and PI results from the multispecimen PI experiments; R^2 is the correlation coefficient of the linear regression; IEF is the intensity error fraction (%).

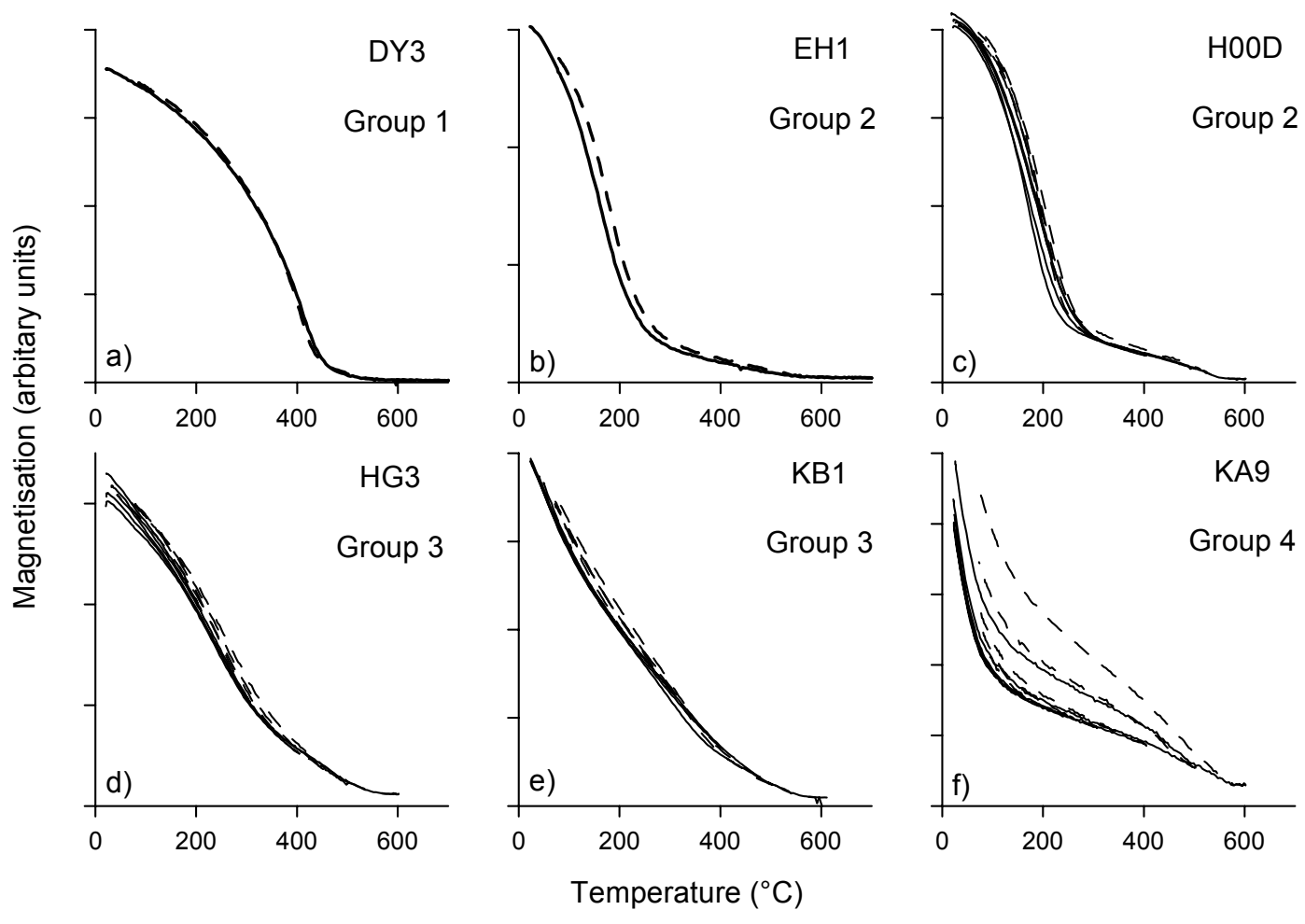
Site	Actual Field (IGRF) (μT)	Multi-specimen PI (μT)	pTRM acquisition at T ($^{\circ}\text{C}$)	R^2	IEF (%)	Thellier estimate (μT)	success rate	IEF (%)
H00	52	60 ± 5	280	0.86	$+15 \pm 10$	62 ± 2	3/4	$+19 \pm 4$
		61 ± 6	200	0.83	$+17 \pm 12$			
H91	52	48 ± 4	280	0.79	-8 ± 8	na	na	
HB	52	54 ± 3	200	0.93	$+4 \pm 6$	60 ± 4	1/5	$+15 \pm 7$
HG	52	57 ± 8	280	0.70	$+10 \pm 15$	43 ± 7	4/5	-17 ± 13
HE	*52	51 ± 7	300	0.71	-2 ± 13	46 ± 7	2/5	-11 ± 13
KA	52	64 ± 3	130	0.96	$+23 \pm 6$	na	na	
KB	*53	58.8 ± 1.2	130	0.97	$+11 \pm 2$	FAIL	0/4	
BK	45	47.1 ± 1.4	280	0.98	$+4 \pm 3$	na	na	
EH	*48	54 ± 6	300	0.78	$+13 \pm 12$	na	na	
EE	**50	65 ± 6	300	0.83	$+30 \pm 12$	na	na	
DY	**47	61.6 ± 1.3	400	0.98	$+31 \pm 3$	na	na	

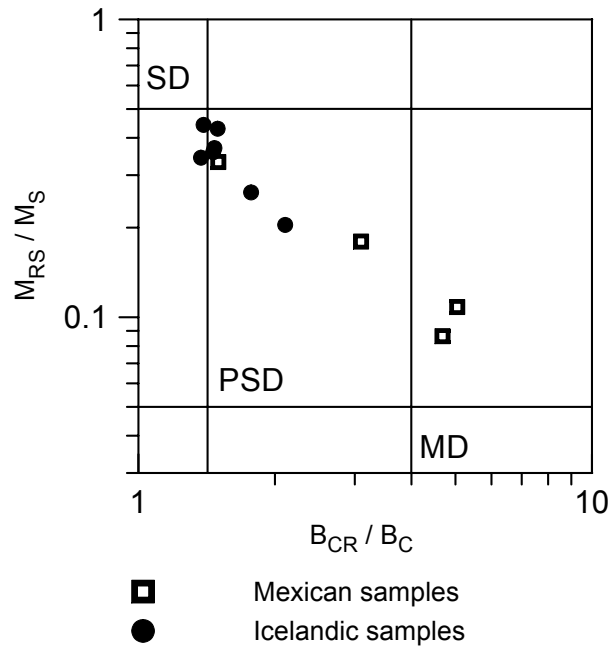
* field estimates for the pre-1900 flows were calculated after the model of Jackson et al., (2000).

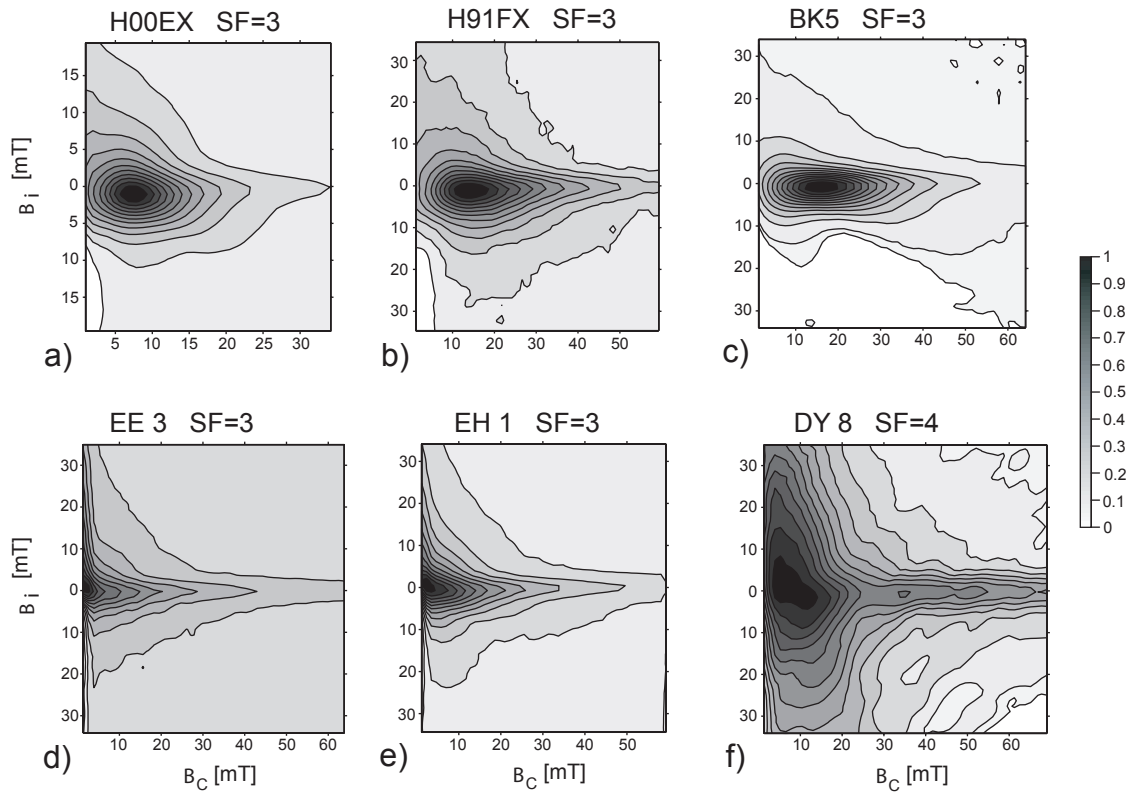
** field estimates were extrapolated from 1590 values using secular variation rates (Jackson et al., 2000) of $0.112 \mu\text{T}/\text{year}$ (EE) and $0.118 \mu\text{T}/\text{year}$ (DY).

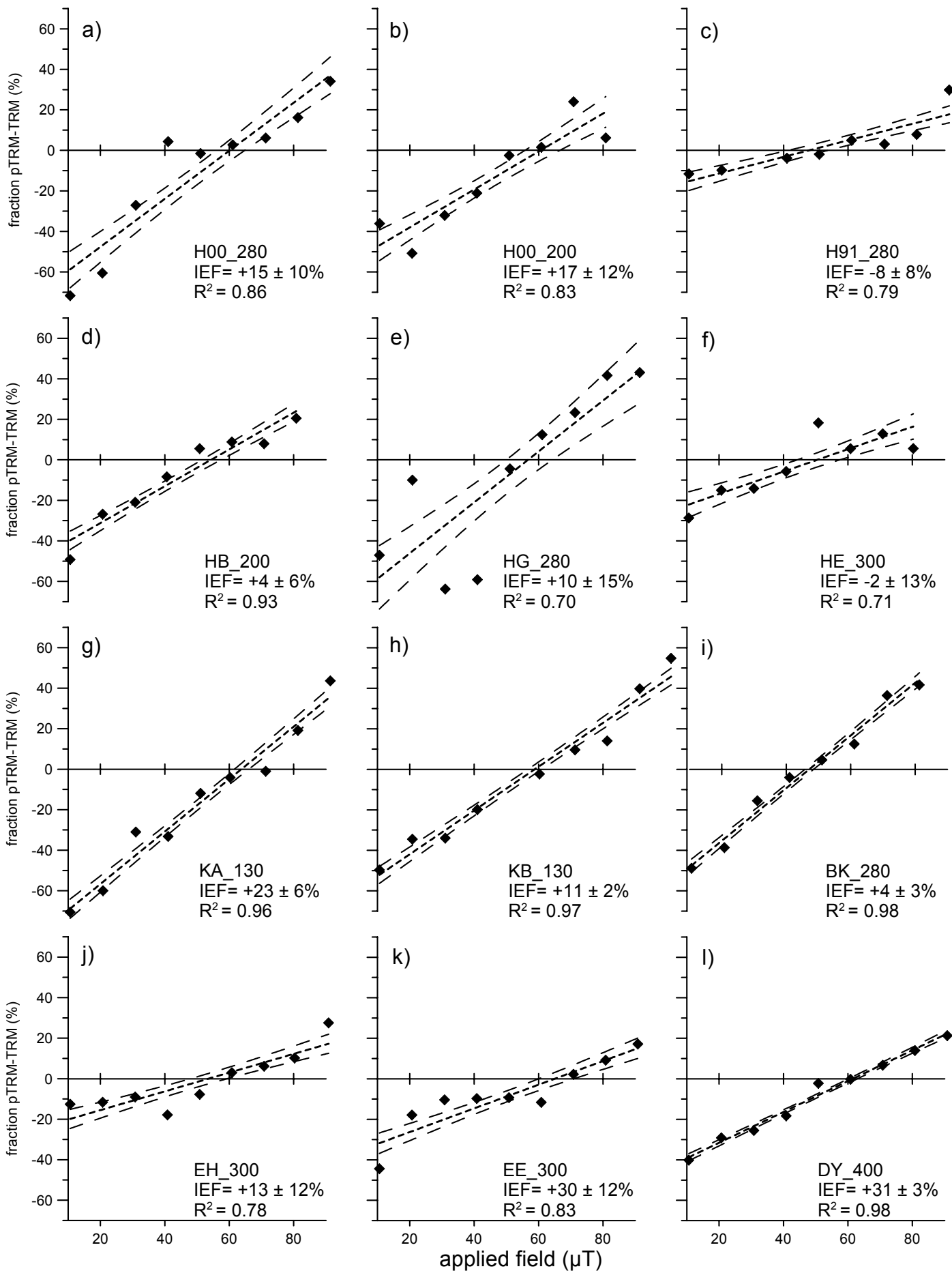
Table 4. Results of the Thellier-type palaeointensity experiment after the IZZI protocol. n/N shows successful versus attempted determinations; H is the palaeointensity value with associated standard deviation (S.D.); H_{exp} is the expected field intensity; IEF is the intensity error fraction; T_{min} and T_{max} denote the temperature range of the straight line segment calculated over N successive points; the fraction of NRM (f), the gap factor (g), the quality factor (q), calculated after Coe et al. (1978); w denotes the weighting factor (Prévot et al., 1985); the class is assigned by the determination criteria of Leonhardt et al., 2004; δ (CK) is the difference between pTRM*- check and repeated pTRM acquisition normalized to the TRM; Drat, like δ (CK) but normalized to the length of the selected segment (Selkin & Tauxe, 2000); $\delta(t^*)$ is the relative extend of the true tail according to Leonhardt et al., 2004 and δ (TR) is the intensity difference of first and repeated demagnetization step normalized to NRMt.

site	n/N	Specimen	H \pm S.D. (μ T)	H exp.	IEF (%)	Tmin	Tmax	N	f	g	q	w	Class	δ (CK)	CK-diff	Drat	$\delta(t^*)$	δ (TR)
H00	3/4	AZ	61.23 \pm 0.81	52	19	100	300	5	0.62	0.69	32.3	18.7	B	4.3	3.6	4.5	3.8	2.6
		BX	63.83 \pm 2.71	52	23	0	300	6	0.65	0.74	11.4	5.7	A	4.4	4.9	4.2	0	2.4
		BY	59.97 \pm 1.38	52	15	100	300	5	0.55	0.62	15.0	8.6	B	4.8	7.8	5.7	0	2.4
HB	1/5	4X	60.44 \pm 3.84	52	15	0	300	6	0.97	0.48	7.4	3.7	B	6.9	7.7	4.6	2.0	0.8
HE	2/5	2Y	49.46 \pm 3.46	52	-5	0	300	6	0.34	0.59	2.8	1.4	B	5.2	3.8	11.0	0	1.4
		7X	42.80 \pm 2.01	52	-18	0	340	7	0.60	0.71	9.0	4.0	B	7.0	9.6	8.9	1.1	1.0
HG	4/5	12X	33.38 \pm 1.36	52	-26	100	340	6	0.62	0.72	11.0	5.5	A	4.1	0.1	5.6	0	4.3
		12Y	48.53 \pm 2.58	52	-7	0	300	6	0.60	0.78	8.8	4.4	A	2.1	3.4	2.5	0.7	1.4
		13X	45.45 \pm 0.95	52	-13	0	300	6	0.63	0.78	23.6	11.8	A	2.5	0.1	3.0	0.2	0.7
		14Y	45.90 \pm 1.08	52	-12	0	340	7	0.86	0.78	28.5	12.7	A	3.8	4.7	3.2	0	2.6

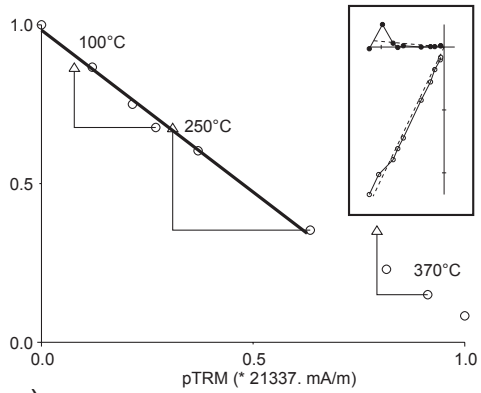






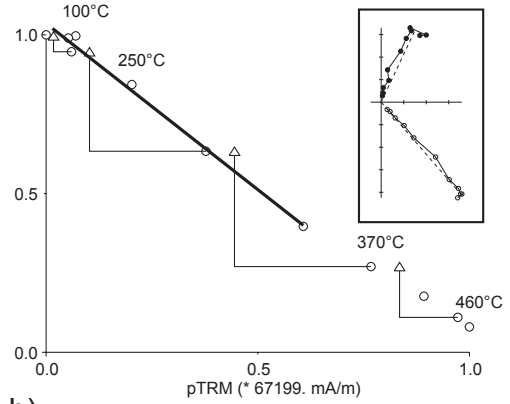


H00BX
 $63.83 \pm 2.71 \mu\text{T}$, IEF= +23%



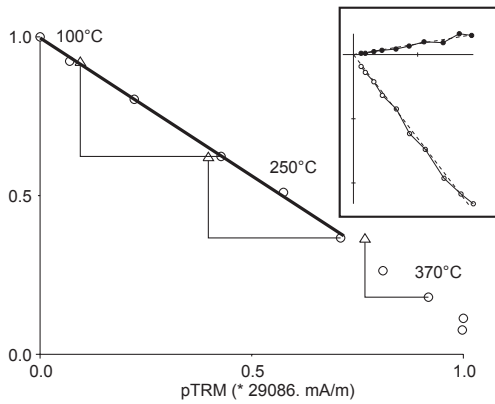
a)

HE7X
 $42.80 \pm 2.01 \mu\text{T}$, IEF= -18%



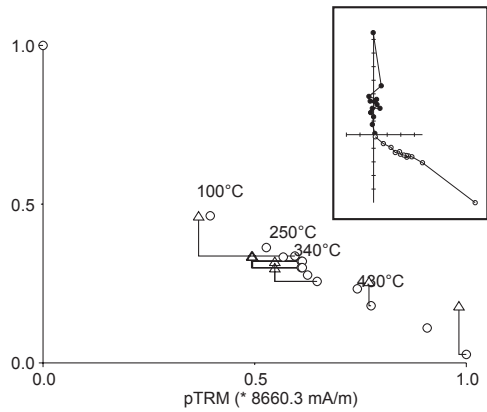
b)

HG13X
 $45.45 \pm 0.95 \mu\text{T}$, IEF= -13%



c)

KB1X
 failed



d)

